ISTITUTO NAZIONALE DI FISICA NUCLEARE

Sezione di Trieste

INFN/BE-93/05

26 ottobre 1993

E. Milotti

RADIATIVE TRANSITIONS IN MUONIC HYDROGEN (revised)

Servizio Documentazione
dei Laboratori Nazionali di Frascati

RADIATIVE TRANSITIONS IN MUONIC HYDROGEN (revised)

Edoardo Milotti

Dipartimento di Fisica dell'Università di Trieste
and
Istituto Nazionale di Fisica Nucleare
Sezione di Trieste, Via Valerio 2, I-34127 Trieste, Italy

Abstract

Recently a new experimental proposal has been put forward to observe and measure the level shifts in muonic hydrogen. Extensive calculations have been carried out in the frame of this experiment to find out the most suitable transitions. This note reports the results of these calculations, and replaces a previous version which contained many errors and misprints.

1. Introduction

The splittings of the atomic energy levels of muonic hydrogen - i.e. the μ^-p bound system - are largely due to the polarization of QED vacuum with electron-positron loops, therefore a measurement of these splittings provides an accurate test of QED.

It is not possible to measure the splittings with a spectroscopic instrument, since a resolution $\frac{\lambda}{\delta\lambda} \approx 10^4 \div 10^6$ in the soft X-ray domain would be required just to detect them. For this reason there have been attempts to measure the splittings with the double resonance method [1]. However one needs an exceedingly powerful far-infrared (FIR) source to induce the transitions and those experiments did not reach their initial goals.

Recently, new powerful electromagnetic radiation sources have become available, and a new experimental proposal has been put forward [2]. Extensive calculations have been carried out in the frame of this experiment to find the most suitable transitions. This note reports the results of these calculations.

All the calculations have been carried out with the Schrödinger wavefunctions and using first-order perturbation theory only; more exact calculations exist [3], but they are not always readily available or so extensive as needed. The values of the physical constants that are needed at some point of the procedure are given in table 1 [4].

The binding energies from the simple Balmer formula up to n = 14 are given in table 2. I stopped at n = 14 because at this n the average radii of the radial muonic wavefunction and of the electronic wavefunction coincide, and detailed Monte Carlo calculations confirm that the muons are captured at n ≈ 14 [5]. Moreover when a muon is captured in a hydrogen gas target it can be shown that Stark mixing due to collisions with the neighbouring molecules is more probable than the radiative transitions for n > 5 at low pressures [6], therefore all the other listings in this note stop at n ≤ 5.

2. Lifetimes

The radiative transition probabilities per unit time for transitions (n,l) -> (n',l±1) have been calculated from the formulas of paragraph 59 of ref. [7], and are listed in table 3. These are the transition probabilities for the electric dipole matrix element, and account nearly for the whole width of each level. Thus the lifetime τ of a certain level is given by

$$\frac{1}{\tau} \approx \Gamma_1 + \Gamma_2 + \ldots = \Gamma \tag{1}$$

where the Γ_i's are the transition probabilities per unit time for the transitions (n,l) -> (n',l±1) associated to that level, and Γ is its width. These lifetimes are listed in table 4. Table 3 lists also the intensity of each line obtained as the product $\hbar\omega_i\Gamma_i$ (see [7]).

3. Level shifts

The realization that muonic atoms may provide useful insights is an old one, and the theoretical calculations that were scattered in several papers have been collected in the review paper by Borie and Rinker [3]. The formulas in this paper have been used to compute the QED corrections, while for the fine structure and hyperfine structure corrections formulas in [7] have been used.

Neglecting the proton electromagnetic structure, and using the notation of [3], the Ühling-Serber potential [8,3] is given by

$$V_{VP1}(r) = -\frac{2\alpha}{3\pi}\frac{Z\alpha}{r}\chi_1(2m_e r) \tag{2}$$

where

$$\chi_1(x) = \int_1^\infty dz\, \frac{\sqrt{z^2-1}}{z^2}\left(1+\frac{1}{2z^2}\right)e^{-xz} \tag{3}$$

Formulas (3) and (2) have been computed numerically, and then the potential (2) has been used to find the order-α QED level shifts from first-order perturbation theory.

The function $\chi_1(x)$ has been computed both by direct integration of (3) and from the Klarsfeld formula [9]

$$\chi_1(x) = \left(1+\frac{x^2}{12}\right)K_0(x) - \left(\frac{5x}{6}+\frac{x^3}{12}\right)K_1(x) + \left(\frac{3x}{4}+\frac{x^3}{12}\right)\int_0^{\pi/2} d\theta\; e^{-z/\cos\theta} \tag{4}$$

where the $K_i(x)$ are modified Bessel functions, with identical results.

For the Källen-Sabry potential the asymptotic expression for large r has been utilized [3]:

$$V_{VP2}(r) \approx \alpha^2\frac{Z\alpha}{r}\frac{e^{-2m_e r}}{m_e r}\left(\frac{8}{\pi^2}\log^2 2 - \frac{1}{4}\right). \tag{5}$$

The numerical results for these four corrections are listed in tables 5 and 6.

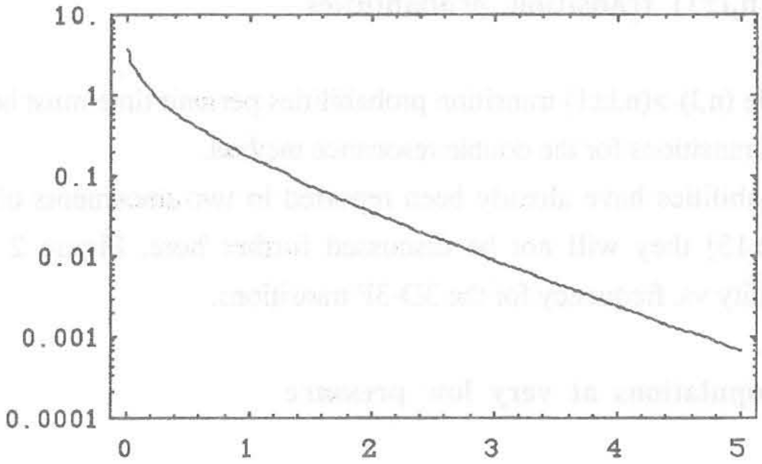

Figure 1: Plot of $\chi_1(x)$ vs. x.

4. Other corrections

There are two noteworthy corrections that have not been included in the calculation of the level shifts, since they are very much smaller than those listed above, namely, the Lamb shift and the finite size corrections. An extensive theoretical discussion can be found in [3,10,11,12].

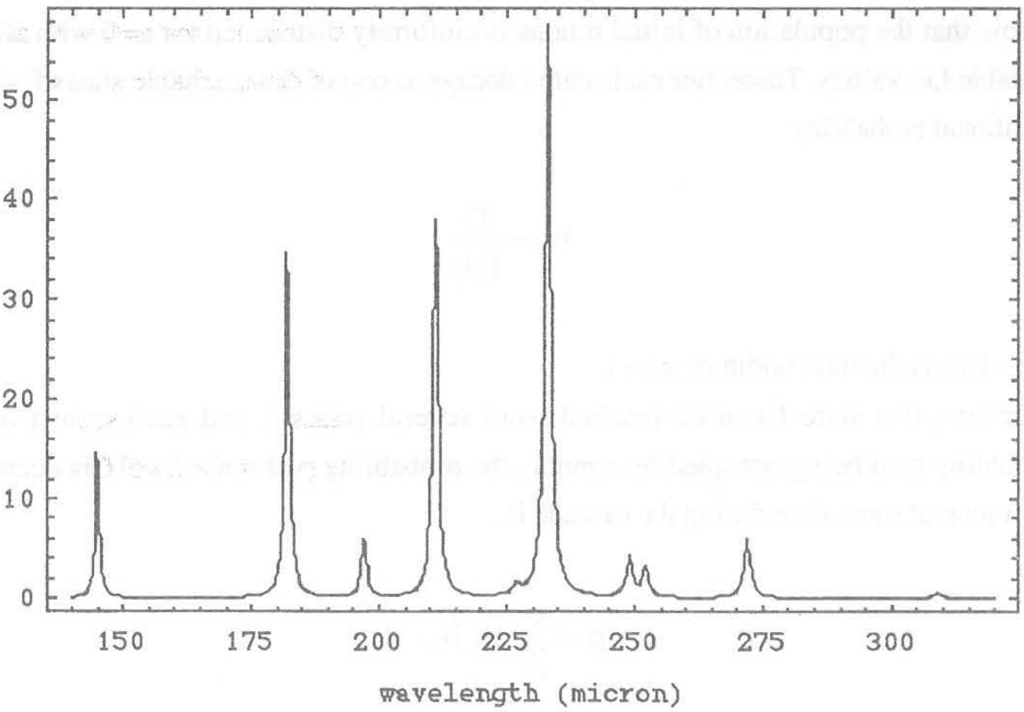

Figure 2: Transition probability (arbitrary units) vs. frequency for the 3D-3P transitions

5. The (n,l)->(n,l±1) transition probabilities

The electric dipole (n,l)->(n,l±1) transition probabilities per unit time must be evaluated to find the "best" transitions for the double resonance method.

Since these probabilities have already been reported in two documents of the MUH Collaboration [2,13] they will not be discussed further here. Figure 2 shows the transition probability vs. frequency for the 3D-3P transitions.

6. Statistical populations at very low pressure

As mentioned in the introduction, the transitions between levels are influenced by Stark mixing, due to collisions with gas molecules, but unfortunately it is difficult to evaluate the transition rates for this Stokes mixing at different gas pressures. A (partial) Markov chain for the stochastic description of the cascade is shown in figure 3 (see also [6]).

Stark mixing introduces loops in the Markov chain of the cascade and this makes an analytical evaluation of the populations impractical. However, if one neglects the Stark mixing it is straightforward to calculate the statistical populations of the different levels from the transition probabilities per unit time Γ_i defined in section 2. Stark mixing becomes negligible at very low gas pressures (<30 mbar) [6] for n < 6: thus one can assume that the population of initial muons is uniformly distributed for n=6 with all the available l,m values. Thereafter each state i decays to one of the reachable states f with a conditional probability

$$B_{if} = \frac{\Gamma_f}{\Gamma(i)} \tag{6}$$

where $\Gamma(i)$ is the total width of state i.

Therefore, if a state f can be reached from several states i, and each state i has a probability p_i of being occupied by a muon, the probability p_f that the level f is occupied by a muon at some time during the cascade is:

$$p_f = \sum_{\{i\}} p_i \, B_{if} \tag{7}$$

The results of this simplified calculation are listed in table 9, and they are in good agreement with a Monte Carlo code developed by Borie and Leon [14].

Still another statistical factor must be included when dealing with the hyperfine components of each line: then if one assumes a uniform distribution among the hyperfine sublevels, the relative abundances in each sublevel are those given in table 10.

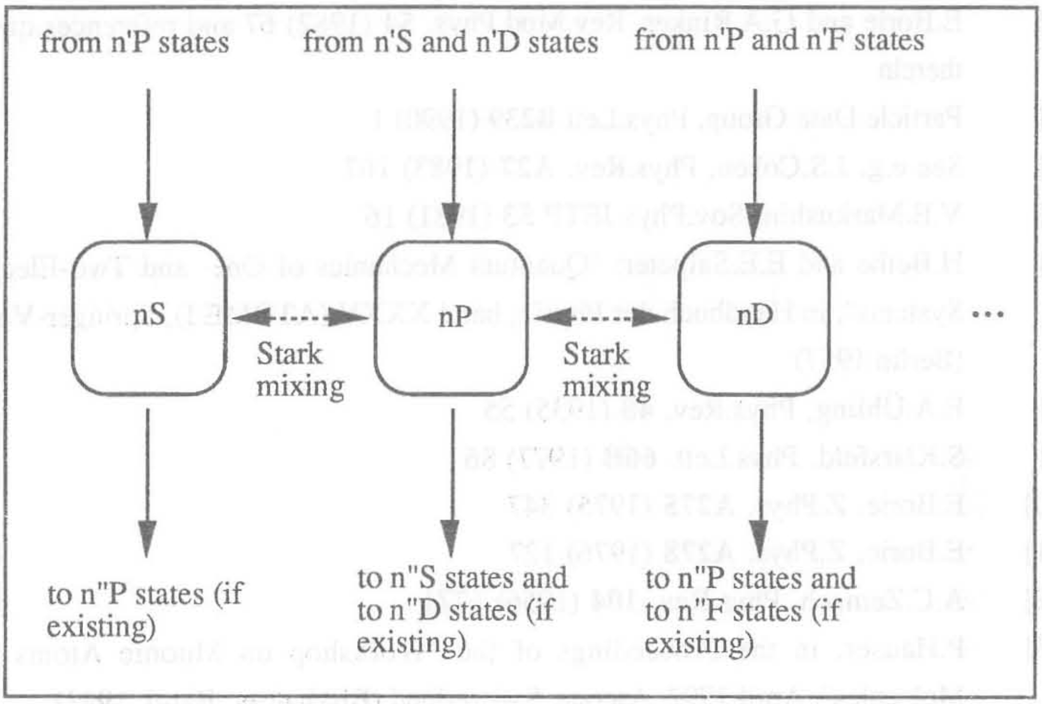

Figure 3: Partial Markov chain description of the cascade

Acknowledgement

I wish to thank Prof. E. Zavattini, who is the real originator of the experimental project [2], for the fruitful discussions and advice.

References

[1] See e.g. H.Anderhub et al., Phys.Lett. **60B** (1976) 273

[2] P.S.I. Proposal R-93-06.1, "3D-3P transition muonic hydrogen" (May 1993) and the invited paper presented by E.Zavattini at the "Workshop on Muonic Atoms and Molecules", April 1992, Ascona, Switzerland (Birkhaüser, Basel 1993)

[3] E.Borie and G.A.Rinker, Rev.Mod.Phys. **54** (1982) 67 and references quoted therein

[4] Particle Data Group, Phys.Lett **B239** (1990) 1

[5] See e.g. J.S.Cohen, Phys.Rev. **A27** (1983) 167

[6] V.E.Markushin, Sov.Phys.JETP **53** (1981) 16

[7] H.Bethe and E.E.Salpeter: "Quantum Mechanics of One- and Two-Electron Systems", in Handbuch der Physik, band XXXV (ATOME I), Springer-Verlag (Berlin 1957)

[8] E.A.Ühling, Phys.Rev. **48** (1935) 55

[9] S.Klarsfeld, Phys.Lett. **66B** (1977) 86

[10] E.Borie, Z.Phys. **A275** (1975) 347

[11] E.Borie, Z.Phys. **A278** (1976) 127

[12] A.C.Zemach, Phys.Rev. **104** (1956) 1771

[13] P.Hauser, in the Proceedings of the "Workshop on Muonic Atoms and Molecules", April 1992, Ascona, Switzerland (Birkhaüser, Basel 1993)

[14] E.Borie and M.Leon, Phys.Rev. **A21** (1980) 1460

Table 1: Constants

Physical constants	
Rydberg Frequency	$3.28985*10^{15}$ Hz
Rydberg Energy	13.6056981 eV
Proton Mass	938.27231 10^6 eV
Proton Gyromagnetic Ratio	2*2.7928474
Electron Mass	0.51099906 10^6 eV
Muon Mass	105.658387 10^6 eV
α	1/137.0359895
Conversion factors	
Hz to eV	4.13567 10^{-15} eV/Hz
eV to Hz	2.41799 10^{14} Hz/eV
Hz to μm	$3*10^{14}$ Hz*μm
eV to μm	1.2407 eV*μm

Table 2: Binding energies from the Balmer formula

n	energy (eV)
1	-2528.
2	-632.1
3	-280.9
4	-158.0
5	-101.1
6	-70.24
7	-51.60
8	-39.51
9	-31.22
10	-25.28
11	-20.90
12	-17.56
13	-14.96
14	-12.90

Table 3: Electric dipole transition probabilities (n,l)->(n,l±1) per unit time

transition	Γ (GHz)	intensity (erg s^{-1})
5G-4F	0.791768	0.000388868
2P-1S	116.6	1.90888
3S-2P	1.17506	0.00356243
3P-1S	31.1283	0.603983
3P-2S	4.17797	0.0126664
3D-2P	12.0326	0.0364793
4S-2P	0.479834	0.00196387
4S-3P	0.341601	0.000362473
4P-1S	12.6906	0.259701
4P-2S	1.79938	0.00736452
4P-3S	0.570467	0.000605323
4P-3D	0.0646819	0.000068634
4D-2P	3.83867	0.015711
4D-3P	1.30981	0.00138984
4F-3D	2.56615	0.00272295
5S-2P	0.239833	0.00109938
5S-3P	0.168377	0.000261361
5S-4P	0.120058	0.0000589651
5P-1S	6.39778	0.134067
5P-2S	0.920959	0.00422163
5P-3S	0.304804	0.000473129
5P-3D	0.0278309	0.0000432002
5P-4S	0.137202	0.000067385
5P-4D	0.035075	0.0000172267
5D-2P	1.75421	0.00804121
5D-3P	0.631205	0.000979781
5D-4P	0.276528	0.000135813
5D-4F	0.00939452	$4.614\ 10^{-6}$
5F-3D	0.845364	0.00131221
5F-4D	0.480999	0.000236237

Table 4: Lifetimes

level	lifetime (ps)
3S	851.
3P	28.3
3D	83.1
4S	1220.
2P	8.58
4P	66.1
4D	194.
4F	390.
5S	1890.
5P	128.
5D	374.
5F	754.
5G	1260.

Table 5: FS, HFS and QED corrections (in meV)

transition	FS	HFS	Ühling	Källen	Total
$2S^{1}_{1/2}-2P^{1}_{1/2}$	0.	-12.69	-205.	-1.203	-218.9
$2S^{1}_{1/2}-2P^{3}_{3/2}$	-8.415	-16.92	-205.	-1.203	-231.5
$2S^{1}_{1/2}-2P^{3}_{1/2}$	0.	-21.14	-205.	-1.203	-227.4
$2S^{3}_{1/2}-2P^{1}_{1/2}$	0.	12.69	-205.	-1.203	-193.5
$2S^{3}_{1/2}-2P^{3}_{3/2}$	-8.415	8.458	-205.	-1.203	-206.2
$2S^{3}_{1/2}-2P^{3}_{1/2}$	0.	4.229	-205.	-1.203	-202.
$2S^{3}_{1/2}-2P^{5}_{3/2}$	-8.415	5.075	-205.	-1.203	-209.6
$3S^{1}_{1/2}-3P^{1}_{1/2}$	0.	-3.759	-59.51	-0.3489	-63.61
$3S^{1}_{1/2}-3P^{3}_{3/2}$	-2.493	-5.012	-59.51	-0.3489	-67.36
$3S^{1}_{1/2}-3P^{3}_{1/2}$	0.	-6.265	-59.51	-0.3489	-66.12
$3S^{3}_{1/2}-3P^{1}_{1/2}$	0.	3.759	-59.51	-0.3489	-56.1
$3S^{3}_{1/2}-3P^{3}_{3/2}$	-2.493	2.506	-59.51	-0.3489	-59.84
$3S^{3}_{1/2}-3P^{3}_{1/2}$	0.	1.253	-59.51	-0.3489	-58.6
$3S^{3}_{1/2}-3P^{5}_{3/2}$	-2.493	1.504	-59.51	-0.3489	-60.85
$3P^{1}_{1/2}-3D^{3}_{3/2}$	-2.493	-1.504	-4.649	-0.03061	-8.677
$3P^{3}_{3/2}-3D^{3}_{3/2}$	0.	-0.2506	-4.649	-0.03061	-4.931
$3P^{3}_{3/2}-3D^{5}_{5/2}$	-0.8311	-0.401	-4.649	-0.03061	-5.912
$3P^{3}_{3/2}-3D^{5}_{3/2}$	0.	-0.852	-4.649	-0.03061	-5.532
$3P^{3}_{1/2}-3D^{3}_{3/2}$	-2.493	1.002	-4.649	-0.03061	-6.171
$3P^{3}_{1/2}-3D^{5}_{3/2}$	-2.493	0.401	-4.649	-0.03061	-6.773
$3P^{7}_{3/2}-3D^{3}_{3/2}$	0.	0.7518	-4.649	-0.03061	-3.928
$3P^{7}_{3/2}-3D^{5}_{5/2}$	-0.8311	0.6014	-4.649	-0.03061	-4.91
$3P^{7}_{3/2}-3D^{5}_{3/2}$	0.	0.1504	-4.649	-0.03061	-4.53
$3P^{7}_{3/2}-3D^{7}_{5/2}$	-0.8311	0.2148	-4.649	-0.03061	-5.296
$4S^{1}_{1/2}-4P^{1}_{1/2}$	0.	-1.586	-24.93	-0.1462	-26.66
$4S^{1}_{1/2}-4P^{3}_{3/2}$	-1.052	-2.114	-24.93	-0.1462	-28.24

Table 5 (ctd.): FS, HFS and QED corrections (in meV)

transition	FS	HFS	Ühling	Källen	Total
$4S^{1}_{1/2}$ - $4P^{3}_{1/2}$	0.	-2.643	-24.93	-0.1462	-27.72
$4S^{3}_{1/2}$ - $4P^{1}_{1/2}$	0.	1.586	-24.93	-0.1462	-23.49
$4S^{3}_{1/2}$ - $4P^{3}_{3/2}$	-1.052	1.057	-24.93	-0.1462	-25.07
$4S^{3}_{1/2}$ - $4P^{3}_{1/2}$	0.	0.5286	-24.93	-0.1462	-24.55
$4S^{3}_{1/2}$ - $4P^{5}_{3/2}$	-1.052	0.6343	-24.93	-0.1462	-25.49
$4P^{1}_{1/2}$ - $4D^{3}_{3/2}$	-1.052	-0.6343	-2.005	-0.01314	-3.705
$4P^{3}_{3/2}$ - $4D^{3}_{3/2}$	0.	-0.1057	-2.005	-0.01314	-2.124
$4P^{3}_{3/2}$ - $4D^{5}_{5/2}$	-0.3506	-0.1692	-2.005	-0.01314	-2.538
$4P^{3}_{3/2}$ - $4D^{5}_{3/2}$	0.	-0.3595	-2.005	-0.01314	-2.378
$4P^{3}_{1/2}$ - $4D^{3}_{3/2}$	-1.052	0.4229	-2.005	-0.01314	-2.647
$4P^{3}_{1/2}$ - $4D^{5}_{3/2}$	-1.052	0.1692	-2.005	-0.01314	-2.901
$4P^{7}_{3/2}$ - $4D^{3}_{3/2}$	0.	0.3172	-2.005	-0.01314	-1.701
$4P^{7}_{3/2}$ - $4D^{5}_{5/2}$	-0.3506	0.2537	-2.005	-0.01314	-2.115
$4P^{7}_{3/2}$ - $4D^{5}_{3/2}$	0.	0.06343	-2.005	-0.01314	-1.955
$4P^{7}_{3/2}$ - $4D^{7}_{5/2}$	-0.3506	0.09062	-2.005	-0.01314	-2.278
$4D^{3}_{3/2}$ - $4F^{5}_{5/2}$	-0.3506	-0.09062	-0.06752	-0.0005208	-0.5093
$4D^{7}_{5/2}$ - $4F^{5}_{5/2}$	0.	-0.02719	-0.06752	-0.0005208	-0.09523
$4D^{7}_{5/2}$ - $4F^{7}_{7/2}$	-0.1753	-0.0466	-0.06752	-0.0005208	-0.29
$4D^{7}_{5/2}$ - $4F^{7}_{5/2}$	0.	-0.1437	-0.06752	-0.0005208	-0.2117
$4D^{7}_{3/2}$ - $4F^{5}_{5/2}$	-0.3506	0.1631	-0.06752	-0.0005208	-0.2556
$4D^{7}_{3/2}$ - $4F^{7}_{5/2}$	-0.3506	0.0466	-0.06752	-0.0005208	-0.3721
$4D^{7}_{5/2}$ - $4F^{5}_{5/2}$	0.	0.1359	-0.06752	-0.0005208	0.06789
$4D^{7}_{5/2}$ - $4F^{7}_{7/2}$	-0.1753	0.1165	-0.06752	-0.0005208	-0.1268
$4D^{7}_{5/2}$ - $4F^{7}_{5/2}$	0.	0.01942	-0.06752	-0.0005208	-0.04862
$4D^{7}_{5/2}$ - $4F^{9}_{7/2}$	-0.1753	0.03021	-0.06752	-0.0005208	-0.2132

Table 6: Allowed transitions in order of increasing frequency

transition	hν	ν (GHz)	λ (μm)
$4D^{7}_{5/2} - 4F^{7}_{5/2}$	-0.04862	11.7568	25517.1
$4D^{7}_{5/2} - 4F^{5}_{5/2}$	0.06789	16.4154	18275.5
$4D^{5}_{5/2} - 4F^{5}_{5/2}$	-0.09523	23.0257	13028.9
$4D^{7}_{5/2} - 4F^{7}_{7/2}$	-0.1268	30.6721	9780.87
$4D^{5}_{5/2} - 4F^{7}_{5/2}$	-0.2117	51.198	5859.6
$4D^{7}_{5/2} - 4F^{9}_{7/2}$	-0.2132	51.5405	5820.67
$4D^{5}_{3/2} - 4F^{5}_{5/2}$	-0.2556	61.7954	4854.73
$4D^{5}_{5/2} - 4F^{7}_{7/2}$	-0.29	70.1133	4278.79
$4D^{5}_{3/2} - 4F^{7}_{5/2}$	-0.3721	89.9677	3334.53
$4D^{3}_{3/2} - 4F^{5}_{5/2}$	-0.5093	123.148	2436.09
$4P^{5}_{3/2} - 4D^{3}_{3/2}$	-1.701	411.34	729.324
$4P^{5}_{3/2} - 4D^{5}_{3/2}$	-1.955	472.693	634.661
$4P^{5}_{3/2} - 4D^{5}_{5/2}$	-2.115	511.463	586.553
$4P^{3}_{3/2} - 4D^{3}_{3/2}$	-2.124	513.595	584.118
$4P^{5}_{3/2} - 4D^{7}_{5/2}$	-2.278	550.904	544.56
$4P^{3}_{3/2} - 4D^{5}_{3/2}$	-2.378	574.948	521.786
$4P^{3}_{3/2} - 4D^{5}_{5/2}$	-2.538	613.718	488.824
$4P^{3}_{1/2} - 4D^{3}_{3/2}$	-2.647	640.129	468.655
$4P^{3}_{1/2} - 4D^{5}_{3/2}$	-2.901	701.482	427.666
$4P^{1}_{1/2} - 4D^{3}_{3/2}$	-3.705	895.767	334.909
$3P^{5}_{3/2} - 3D^{3}_{3/2}$	-3.928	949.846	315.841
$3P^{5}_{3/2} - 3D^{5}_{3/2}$	-4.53	1095.27	273.904
$3P^{5}_{3/2} - 3D^{5}_{5/2}$	-4.91	1187.17	252.701
$3P^{3}_{3/2} - 3D^{3}_{3/2}$	-4.931	1192.23	251.63
$3P^{5}_{3/2} - 3D^{7}_{5/2}$	-5.296	1280.66	234.254
$3P^{3}_{3/2} - 3D^{5}_{3/2}$	-5.532	1337.66	224.273

Table 6 (ctd.): Allowed transitions in order of increasing frequency

transition	hν	ν (GHz)	λ (μm)
$3P^{3}_{3/2} - 3D^{5}_{5/2}$	-5.912	1429.56	209.855
$3P^{3}_{1/2} - 3D^{3}_{3/2}$	-6.171	1492.16	201.051
$3P^{3}_{1/2} - 3D^{5}_{3/2}$	-6.773	1637.59	183.196
$3P^{1}_{1/2} - 3D^{3}_{3/2}$	-8.677	2098.12	142.985
$4S^{3}_{1/2} - 4P^{1}_{1/2}$	-23.49	5680.19	52.8151
$4S^{3}_{1/2} - 4P^{3}_{1/2}$	-24.55	5935.83	50.5405
$4S^{3}_{1/2} - 4P^{3}_{3/2}$	-25.07	6062.37	49.4856
$4S^{3}_{1/2} - 4P^{5}_{3/2}$	-25.49	6164.62	48.6648
$4S^{1}_{1/2} - 4P^{1}_{1/2}$	-26.66	6447.11	46.5325
$4S^{1}_{1/2} - 4P^{3}_{1/2}$	-27.72	6702.74	44.7578
$4S^{1}_{1/2} - 4P^{3}_{3/2}$	-28.24	6829.28	43.9285
$3S^{3}_{1/2} - 3P^{1}_{1/2}$	-56.1	13564.1	22.1172
$3S^{3}_{1/2} - 3P^{3}_{1/2}$	-58.6	14170.1	21.1714
$3S^{3}_{1/2} - 3P^{3}_{3/2}$	-59.84	14470.	20.7326
$3S^{3}_{1/2} - 3P^{5}_{3/2}$	-60.85	14712.4	20.391
$3S^{1}_{1/2} - 3P^{1}_{1/2}$	-63.61	15382.	19.5034
$3S^{1}_{1/2} - 3P^{3}_{1/2}$	-66.12	15987.9	18.7642
$3S^{1}_{1/2} - 3P^{3}_{3/2}$	-67.36	16287.9	18.4186
$2S^{3}_{1/2} - 2P^{1}_{1/2}$	-193.5	46793.8	6.41111
$2S^{3}_{1/2} - 2P^{3}_{1/2}$	-202.	48838.9	6.14264
$2S^{3}_{1/2} - 2P^{3}_{3/2}$	-206.2	49851.2	6.01791
$2S^{3}_{1/2} - 2P^{5}_{3/2}$	-209.6	50669.2	5.92075
$2S^{1}_{1/2} - 2P^{1}_{1/2}$	-218.9	52929.1	5.66796
$2S^{1}_{1/2} - 2P^{3}_{1/2}$	-227.4	54974.2	5.45711
$2S^{1}_{1/2} - 2P^{3}_{3/2}$	-231.5	55965.4	5.36046

Table 7: Statistical populations at very low gas pressure

nL	% fraction of μ that pass through level
4S	0.2
4P	3.0
4D	10.
4F	36.
3S	0.6
3P	8.7
3D	54.
2S	2.8
2P	77.

Table 8: Statistical populations of hyperfine sublevels

L_j^{2f+1}	% of total population
$S_{1/2}^{1}$	25%
$S_{3/2}^{1}$	75%
$P_{1/2}^{1}$	8.3%
$P_{1/2}^{3}$	25%
$P_{3/2}^{3}$	25%
$P_{3/2}^{5}$	41.7%
$D_{3/2}^{3}$	15%
$D_{3/2}^{5}$	25%
$D_{5/2}^{5}$	25%
$D_{5/2}^{7}$	35%